IEEE Access
Multidisciplinary | Rapid Review | Open Access Journal

Received February 11, 2020, accepted February 25, 2020, date of publication March 2, 2020, date of current version March 31, 2020.

Digital Object Identifier 10.1109/ACCESS.2020.2977630

A Multi-Elements Chessboard Random Coded Metasurface Structure for Ultra-Wideband Radar Cross Section Reduction

HUIJUAN DAI, YONGJIU ZHAO, AND CHEN YU

Key Laboratory of Radar Imaging and Microwave Photonics, Ministry of Education, College of Electronic and Information Engineering, Nanjing University of Aeronautics and Astronautics, Nanjing 210016, China

Corresponding author: Huijuan Dai (daihuijuan519@163.com)

ABSTRACT In this paper, a novel method of realizing the ultra-wideband (UWB) radar cross section (RCS) reduction is proposed. We combine the chessboard structure of multi-elements which are all polarization conversion metasurface (PCM) units with random coding. Four different kinds of PCM units all with UWB and much high polarization conversion rate (PCR) are selected. Morever, their polarization conversion frequency bands are optimized not only in the high frequency segment but also in the low frequency segment. The final designed structure can achieve 10 dB RCS reduction within 6.9 GHz-20.1 GHz in the high frequency segment and 15.5 GHz-51.2 GHz in the low frequency segment, respectively. In addition, the effects of RCS reduction by the square chessboard structure composed of different numbers of these PCM units are compared. The proposed metasurface structure provides an efficient scheme to reduce the scattering of the electromagnetic waves.

INDEX TERMS Chessboard random code metasurface, ultra-wideband (UWB), radar cross section (RCS).

I. INTRODUCTION

In recent years, with the rapid development of radar technology, the theoretical research and practical application of stealth technology has become a hot spot of domestic and foreign scholars. In the future war, radar will still be the most important and reliable means to detect the target. Therefore, the research of stealth technology focuses on the radar characteristic signal control of the target. The essence of radar stealth is to use various means to reduce the echo signal of the target, so that the enemy radar can't detect accurately. The radar cross section (RCS) of a target is the physical quantity that represents the strength of the radar echo of the target. It is the most critical concept in radar detection technology and anti-radar stealth technology [1]. In the use of radar, people tend to pay more attention to the echo with the same polarization as the transmitted electromagnetic wave. If the surface of target can realize polarization conversion and convert the linearly polarized incident wave into the outgoing wave which is perpendicular to its polarization, then for the radar with the same polarization of the receiving and transmitting antennas, the target signal can't be accurately received and the purpose of stealth are achieved. In this case, the PCM [2]–[5], which can achieve high efficiency polarization conversion, will be a very good stealth material.

The mechanism of artificial magnetic conductor (AMC) in chessboard configurations is based on the elimination of interference of the reflected waves generated by the PEC and AMC units that constitute the chessboard structure [6], [7]. To further improve the bandwidth of 10 dB RCS reduction, various methods have been proposed, but with a cost of structural complexities [8]–[10]. Finally, PCM chessboard is proposed to simplify the design by using the same PCM unit to realize a chessboard structure. Since PCM unit can be rotated by 90° and the phase difference between the two structures can be maintained 180° all the time, so the only factor affecting the RCS reduction performance is the PCR [11]. Random surface [12], using the characteristics of diffuse reflection to reduce the RCS of microwave frequency band. By adjusting the reflection phase of the array element, random metasurface makes the reflection phase of each element uniformly and randomly arranged in 360° to scatter the strong reflection peak of the metal target into irregular scattering wave in all directions, so as to significantly reduce the back scattering

The associate editor coordinating the review of this manuscript and approving it for publication was Davide Ramaccia.

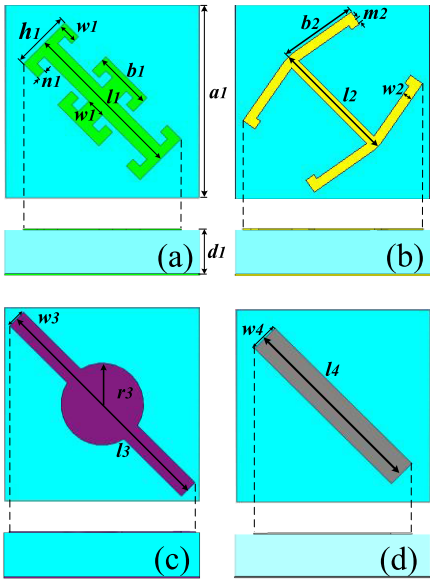

FIGURE 1. Structure diagram of (a) PCM unit 1, (b) PCM unit 2, (c) PCM unit 3, (d) PCM unit 4.

and achieve stealth. In addition, professor Cui Tiejun et al. proposed a new concept of coding metasurface [13]. The coding metasurface is composed of elements with the same phase difference in a broadband, which is basically constant. According to the number of coding bits, there are 1 bit, 2 bit, 3 bit metasurface, and so on. By selecting different coding sequence, arbitrary control of electromagnetic wave can be realized [14].

Therefore, in this paper, a new type of PCM chessboard metasurface with random coding is constructed by the elements with broadband polar- ization conversion property, which can not only scatter the electromagnetic wave in all directions, but also convert the incident electromagnetic wave into another kind of linearly polarized outgoing wave with cross polarization. It greatly widens the backward RCS reduction bandwidth.

II. DESIGN OF THE UNITS AND THEORETICAL ANALYSIS

The four UWB PCM units designed in this paper are shown in Fig.1. In this paper, we call them as PCM unit1, PCM unit2, PCM unit3, PCM unit4. Through the simulation and optimization of CST Microwave Studio, in the high frequency segment, the uniform period size is 4 mm, the chosen dielectric layer is F4B: $\varepsilon_r = 2.2$, $\tan\sigma = 0.001$, and the thickness is 1.5 mm, the other local geometric parameters are shown in Table 1 in the high frequency segment. All of these structures can excite multiple resonance modes to expand the polarization conversion bandwidth. Their −10 dB polarization conversion bandwidths are: 20 GHz-47.7 GHz, 15.4 GHz-50.54 GHz, 16.68 GHz- 50.02 GHz, 20.22 GHz-45.74 GHz, respectively (as shown in Figure 2).

Then, by adjusting the other local geometric parameters and the thickness of the dielectric layer as shown in Table 1 in

TABLE 1. Dimensions of four elements at high frequency segment and low frequency segment.

	low freq. segment (mm)	high freq. segment (mm)
unit 1	w_1=2.7 b_1=h$_1$=1 l_1=6.6 n_1=10	w_1=0.4 b_1=h_1=1 l_1=3 n_1=0.2
unit 2	w_2=n_2=0.6 b_2=3 l_2=6 m_2=0.6 p=80°	w_2=n_2=0.2 b_2=1.5 l_2=2.6 m_2=0.1 p=80°
unit 3	r_3=2 w_3=1 b_3=12	r_3=0.85 w_3=0.4 b_3=5
unit 4	l_4=2.6 w_4=3	l_4=2.6 w_4=0.6

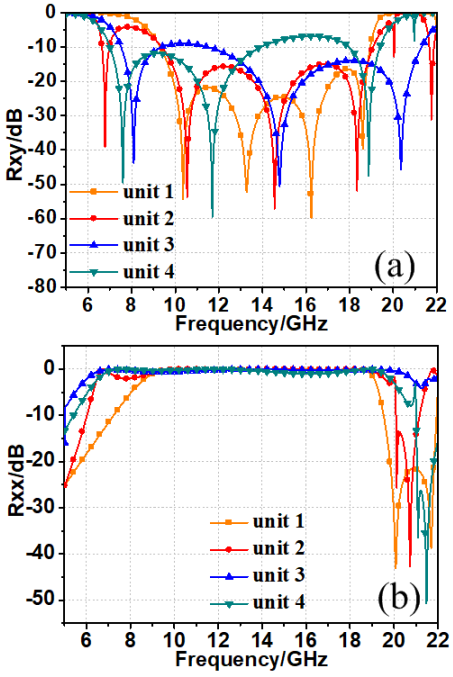

FIGURE 2. Co- and cross-polarization reflection coefficients of four units in the low frequency segment.

the low frequency segment, the four kinds of UWB polarization conversion units are respectively optimized to the low frequency segment, so that the uniform period sizes are 10 mm, the thickness is 3.2 mm, the dielectric layer is F4B: $\varepsilon_r = 2.65$, $\tan\sigma = 0.001$, and their −10 dB polarization conversion bandwidth are 9.3 GHz-19 GHz, 6.7 GHz-19.9 GHz, 7.6 GHz-21.2 GHz and 7 GHz-19.6 GHz. Here, The PCR is defined as PCR= $r_{xy}^2/(r_{xy}^2+r_{yy}^2) = r_{yx}^2/(r_{yx}^2+r_{yy}^2)$ (1), where r_{xy} and r_{yx} represent the cross-polarization reflection coefficients, and r_{xx} and r_{yy} represent the co- polarization reflection coefficients. Figure 2 and Figure 3 show the

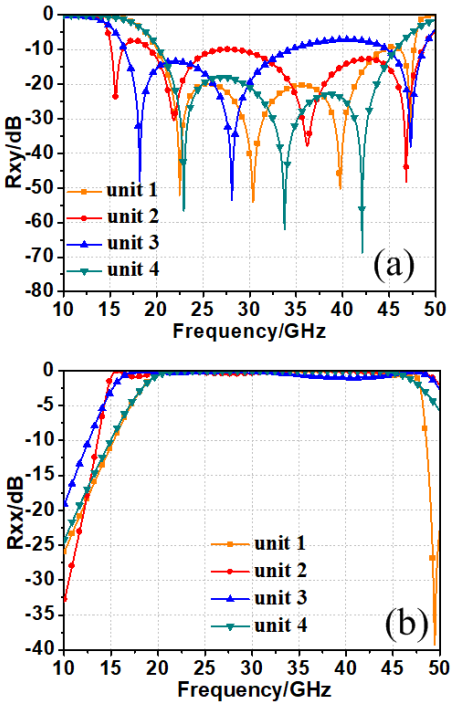

FIGURE 3. Co- and cross-polarization reflection coefficients of four elements in the high frequency segment.

co- and cross-polarization reflection coefficients of the four units in the low frequency segment and in the high frequency segment, respectively. We can observe that the PCR can reach more than 90% between all these −10 dB polarization conversion bandwidth in the low frequency segment and high frequency segment [15].

III. DESIGN AND ANALYSIS OF THE META-SURFACE STRUCTURE

A. COMPARISONS OF RCS REDUCTION EFFECT OF META-SURFACES CONSIST OF DIFFERENT NUMBERS OF PCM UNITS

In the case of the high frequency segment, four different kinds of PCM units above are firstly constructed into 6×6 square chessboard structures respectively, and then combined each of them into 4 × 4 metasurface structures (see in Figure 4a-4d), respectively. For the chessboard structure composed of PCM units, the reflection phase of each part is 180° different from that of the adjacent parts, and the reflection waves of each two parts cancel each other, so the RCS reduction effect is not bad [16]. Secondly, we select two of these four units to form a 6 × 6 chessboard structure respectively, and then arrange these four different chessboard structures into a 4 × 4 metesurface structure (see in Fig. 4e). Then, we choose three of them to form a 6 × 6 chessboard structure, and arrange these chessboard structures into a 4 × 4 structure (see in Fig. 4f). Finally, we use these four different units to form four different 6 × 6 PCM chessboard structures, and then they are arranged into a 4 × 4 structure in the order of ''1234, 2341, 3412, 4123''. (Here, we use the numbers ''1'', ''2'', ''3'' and ''4'' to represent four different 6 × 6 PCM chessboard composed of the four different units, see in Fig. 4g.)

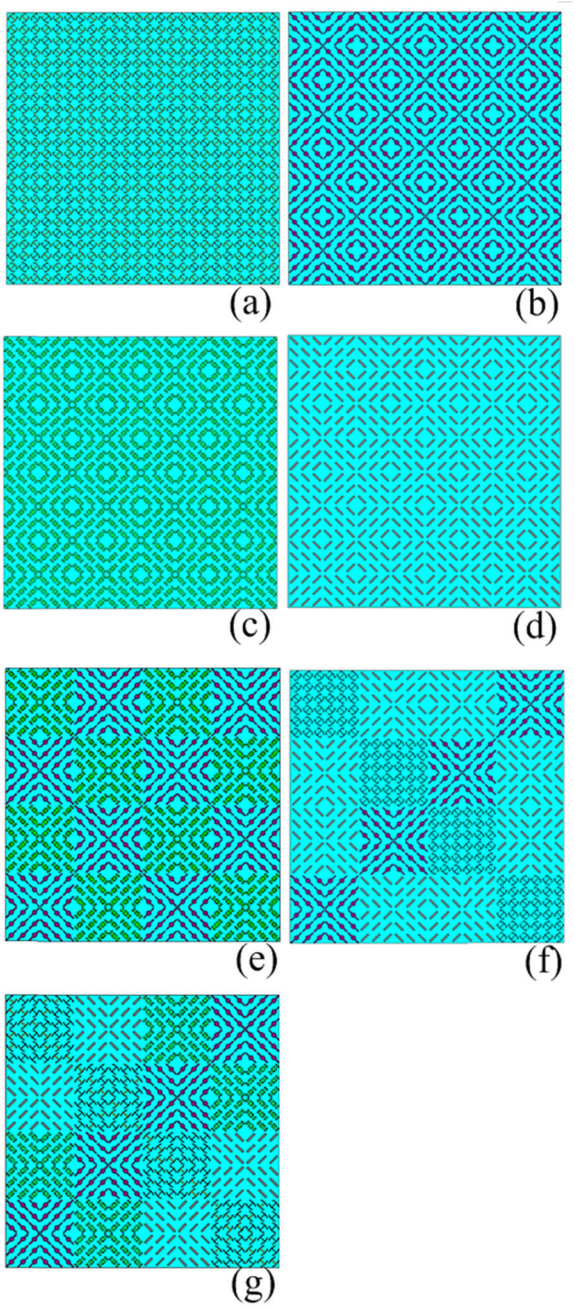

FIGURE 4. Chessboard structure composed of (a) PCM unit1, (b) PCM unit2, (c) PCM unit3, (d) PCM unit4, (e) PCM unit2 and PCM unit3, (f) PCM unit1, PCM unit2 and PCM unit4, (g) these four different PCM units.

The monostatic RCS reduction effect realized by the seven different chessboard structures (see in Fig. 4a-4f) are shown in Fig. 5. The bold red line in Fig. 5 represents the RCS reduction realized by the metasurface of chessboard structure composed of four different PCM units arranged in order (as shown in Fig. 4g). It can be seen clearly that the monostatic RCS reduction effect achieved by the four-elements random

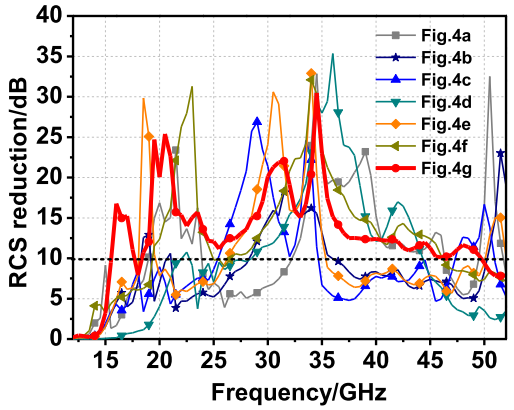

FIGURE 5. The RCS reduction effect realized by the seven different chessboard structures in Figure 4.

coded chessboard structure is the best, which has the widest 10 dB RCS reduction bandwidth. In addition, we have also considered the effect of RCS reduction by choosing other two or three different kinds of PCM to compose chessboard structures with the same size, and the results are consistent with above. In a word, using four different PCM units to form the chessboard structure is better than using one or two or three different PCM units to form the chessboard structure to achieve RCS reduction. (Several other chessboard structures consisted of these two or three PCM units are omitted here, the simulation results show that they are not as good as the structure consisted of four different PCM units, as show in Fig. 4g.)

B. RCS REDUCTION COMPARISONS BETWEEN RANDOM AND ORDERLY CODED METASURFACES

Combining with random coding, the chessboard structure composed of four different elements is arranged according to random coding, and the effect of RCS reduction is further improved. As mentioned above, we use numbers "1", "2", "3" and "4" to represent four different PCM chessboard structures. Fig. 6 (a) is a 6 × 6 chessboard structure composed of the four different units in the order of "1234, 2341, 3412, 4123". Then generate the random sequence according to Matlab software, such as "1411, 3324, 2413, 4231". As shown in Fig. 6 (b), we arrange the four different PCM chessboard structures in the random order above in the high frequency segment. Fig. 6 (c) is the same arrangement as Fig. 6 (b) in the low frequency segment.

Figure7 shows the comparison of RCS reduction between the orderly and random arrangement corresponding to Fig. 6(a) and 6(b). It is obvious that the RCS reduction effect of random coding is better than that of orderly coding metasurface, especially at 19.5 GHz, under the condition of the same sizes and elements. Although only the 4 × 4 random coding is discussed in this paper, with the increasing of the number of coding sequences, the effect of RCS backscatter realized by the structure is better than that of orderly arrangement obviously.

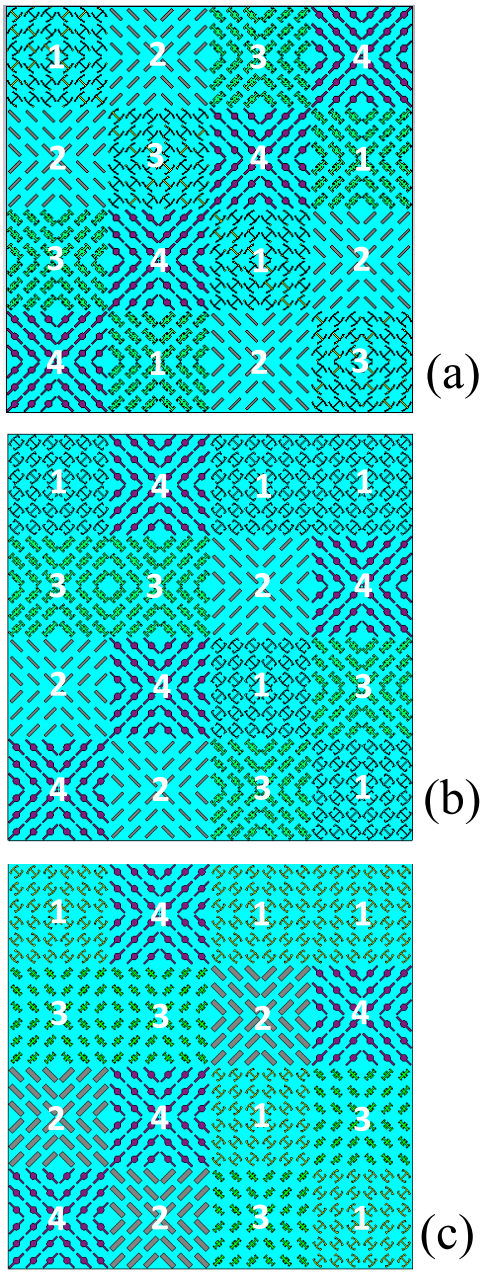

FIGURE 6. The orderly chessboard structure in the high frequency segment, (b) chessboard random coding structure in the high frequency segment, (c) square chessboard random coding structure in the low frequency segment.

Figure 8 shows the simulation far-field patterns of the scattering of the orderly coding chessboard structure and chessboard random coding structure in the high frequency segment, respectively. We can observe from Figure 8a and 8b that the main lobe reduces significantly and many side lobes are produced.

Moreover, the proposed structure with random coding (Figure 8b) is more conducive to realizing RCS reduction with better backscatter, compared with the case in Figure 8a, which is orderly coding structure. As shown in Fig. 9, we can

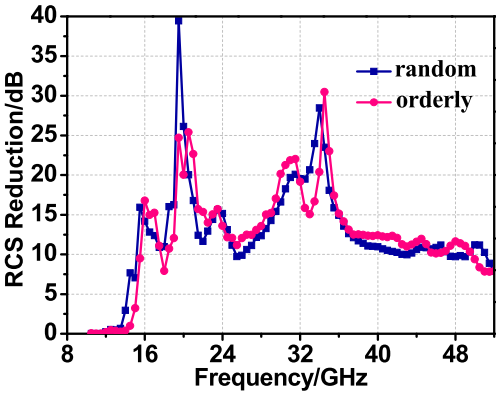

FIGURE 7. Comparison of RCS reduction of the orderly and random arrangement corresponding to Figure 6 (a) and 6(b).

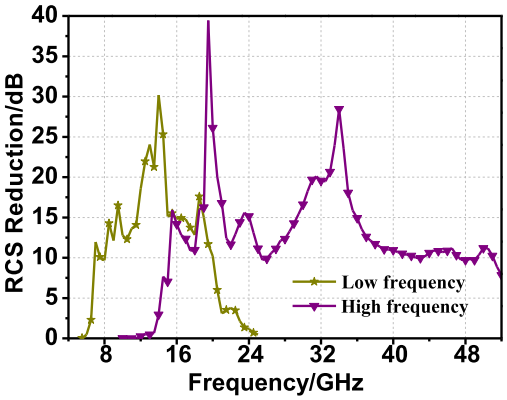

FIGURE 9. RCS reduction results of high frequency part and low frequency segment.

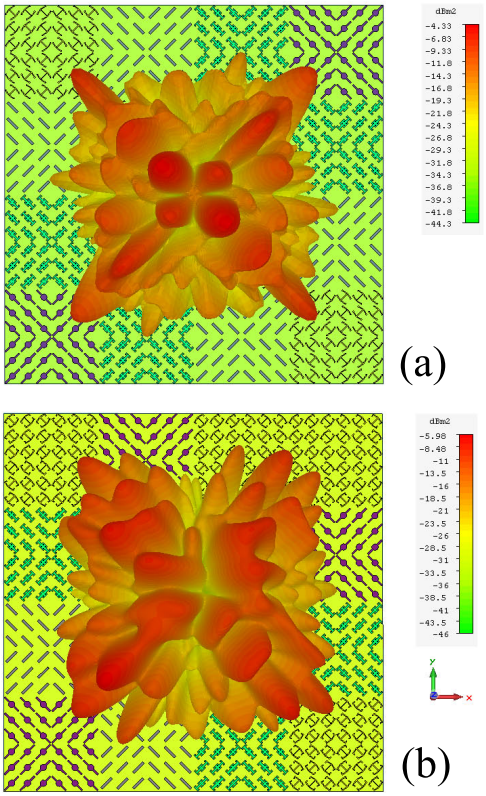

FIGURE 8. Simulation far-field patterns of the scattering in the high frequency segment of (a) chessboard structure in the orderly arrangement at 20.8 GHz, and (b) chessboard in random coding arrangement at 14.0 GHz.

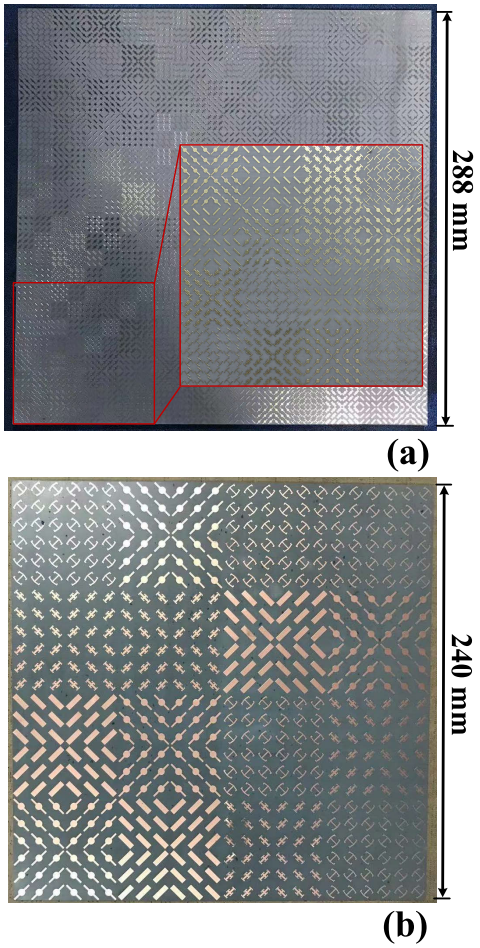

FIGURE 10. The fabricated (a) high frequency segment meta- face and (b) low frequency segment metasurface.

see that this designed structure can achieve 10 dB RCS reduction within 6.9 GHz-20.1 GHz in the low frequency segment, and 15.5 GHz-51.2 GHz in the high frequency segment, respectively. It shows that the UWB structure is not only suitable for high frequency segment, but also for low frequency segment.

IV. EXPERIMENTAL AND FABRICATION

As shown in Fig.10, they are the fabricated prototype of the designed samples. Figure10 (a) is a high-frequency segment sample, with the total size of 288 mm×288 mm, which is three times of the corresponding expansion of simulation model (see in Fig. 5 (b)). (The red box in Fig.10 (a) is an enlarged view of one multi-elements random coding chessboard structure.) Figure 10 (b) shows a low- frequency

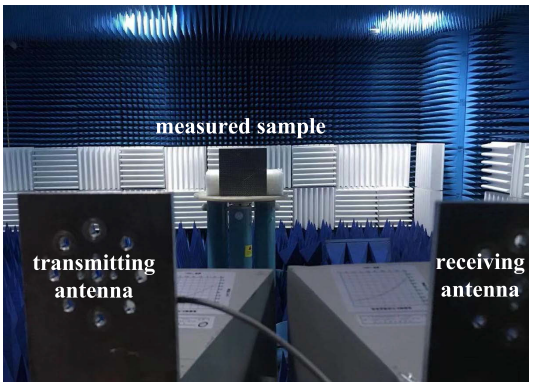

FIGURE 11. Experimental setup for the RCS measurement in an anechoic chamber.

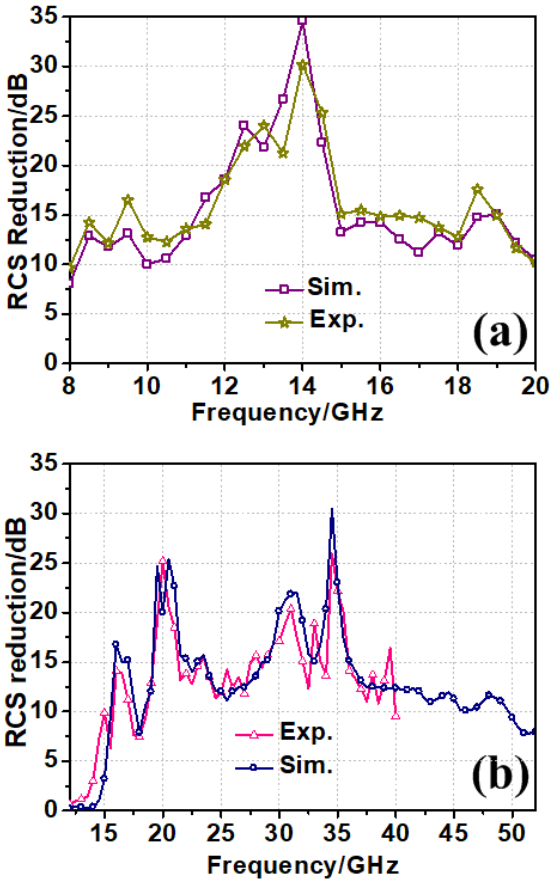

FIGURE 12. Comparison of measurement and simulation results between (a) the low frequency segment and (b) the high frequency segment.

segment sample with a total size of 240 mm × 240 mm, corresponding to the simulation model of Fig. 5(c).

Figure 11 shows the experimental setup in an anechoic chamber. Three pairs of two identical conical horn antennas are used in the experiment, whose frequency bands are: 8 GHz-12.5 GHz, 12 GHz-18 GHz and 18 GHz-40 GHz, respectively. During the test, each pair of horn antennas are used as the transmitter and receiver respectively, and they are respectively fixed on the bracket to form an included angle of less than 5°. The sample to be tested is fixed on the rotary table which is perpendicular to the horizontal plane, and the position of the sample and the two antennas need to be adjusted to ensure that the centers of them are at the same height. Keep a certain distance between the sample and the antennas to meet the far-field test conditions. During the test, the ports of the two antennas are connected to the port1 and port2 of the vector network analyzer (Agilent N5245A).

The experimental test results are shown in Fig. 12. It can be seen that the simulation of RCS reduction effect of samples is basically consistent with the experimental results in the high-frequency and low-frequency segments. There are several possible reasons for some errors: (1) an ideal plane wave is used in simulation while the plane wave used in the experiment is generated by the far-field radiation of the horn antennas; (2) loss errors of vector network analyzer with connecting wires; (3) random errors in measurement and others. (Owing to the limitation of experimental equipment, we can only test the parts below 40 GHz.)

As shown in Table 2, compared with the existing papers on realizing RCS in recent years, the unit size of this paper is smaller and the bandwidth of realizing RCS reduction is wider. [p: unit cell periodicity of the polarization converter, t: dielectric substrate thickness of the polarization converter, OB: operating bandwidth (PCR > 90%), RB: relative bandwidth (PCR > 90%).]

TABLE 2. Comparison with the present state-of-the-art for radar cross section (RCS) reduction.

Ref.	RB (%)	t (mm)	p (mm)
Ref.[17]	49	3	10
Ref.[11]	77	1.6	6.29
Ref.[12]	90.5	1.6	6.4
Ref.[7]	95.9	1.6	6.4
Present study	109	1.5	4

V. CONCLUSION

In this paper, a new multi-elements chessboard random coding metasurface structure for RCS reduction in an UWB has been designed, fabricated and measured. The proposed structure consists of four different kinds of UWB PCM units. In this paper, we ingeniously combine the idea of PCM with the chessboard structure and random coding metasurface to realize UWB RCS reduction. Through the optimization of the local geometric parameters of each element, the thicknesses and types of the dielectric layer, the RCS reduction of the UWB in the low frequency segment (6.9 GHz-20.1 GHz) and the high frequency segment (15.2 GHz-51.2 GHz) are realized, respectively. The experimental results are in good

agreement with the simulation results. The proposed metasurface structure can have potential applications in stealth surfaces, and antennas among others.

REFERENCES

[1] E. F. Knott, "A progression of high-frequency RCS prediction techniques," *Proc. IEEE*, vol. 73, no. 2, pp. 252–264, Feb. 1985.
[2] H. Sun, C. Gu, X. Chen, Z. Li, and F. Martin, "Ultra-wideband and broad-angle linear polarization conversion metasurface," *J. Appl. Phys.*, vol. 121, no. 17, pp. 1304–1404, 2017.
[3] M. Akbari, M. Farahani, A.-R. Sebak, and T. A. Denidni, "Ka-band linear to circular polarization converter based on multilayer slab with broadband performance," *IEEE Access*, vol. 5, pp. 17927–17937, 2017.
[4] M. Akbari, H. A. Ghalyon, M. Farahani, A.-R. Sebak, and T. A. Denidni, "Spatially decoupling of CP antennas based on FSS for 30-GHz MIMO systems," *IEEE Access*, vol. 5, pp. 6527–6537, 2017.
[5] E. Ameri, S. Esmaeli, and S. Sedighy, "Ultra wideband radar cross section reduction by using polarization conversion metasurfaces," *Sci. Rep.*, vol. 9, p. 478, Jan. 2019.
[6] M. Paquay, J.-C. Iriarte, I. Ederra, R. Gonzalo, and P. de Maagt, "Thin AMC structure for radar cross-section reduction," *IEEE Trans. Antennas Propag.*, vol. 55, no. 12, pp. 3630–3638, Dec. 2007.
[7] H. Dai, Y. Zhao, J. Chen, C. Yu, L. Xing, "Ultra-wideband radar cross-section reduction using polarization conversion metasurface," *Int. J. RF Microw. Comput.-Aided Eng.*, vol. 30, no. 2, Feb. 2020, Art. no. e22085.
[8] J. C. Iriarte Galarregui, A. Tellechea Pereda, J. L. M. de Falcon, I. Ederra, R. Gonzalo, and P. de Maagt, "Broadband radar cross-section reduction using AMC technology," *IEEE Trans. Antennas Propag.*, vol. 61, no. 12, pp. 6136–6143, Dec. 2013.
[9] A. Edalati and K. Sarabandi, "Wideband, wide angle, polarization independent RCS reduction using nonabsorptive miniaturized-element frequency selective surfaces," *IEEE Trans. Antennas Propag.*, vol. 62, no. 2, pp. 747–754, Feb. 2014.
[10] Y. Q. Zhuang, G.-M. Wang, and H.-X. Xu, "Ultra-wideband RCS reduction using novel configured chessboard metasurface," *Chin. Phys. B*, vol. 26, no. 5, pp. 113–119, 2017.
[11] X. Gao, X. Han, W. P. Cao, H. O. Li, H. F. Ma, and T. J. Cui, "Ultrawideband and high-efficiency linear polarization converter based on double V-shaped metasurface," *IEEE Trans. Antennas Propag.*, vol. 63, no. 8, pp. 3522–3530, Aug. 2015.
[12] P. Su, Y. Zhao, S. Jia, W. Shi, and H. Wang, "An ultra-wideband and polarization-independent metasurface for RCS reduction," *Sci. Rep.*, vol. 6, p. 20387, Feb. 2016.
[13] T. J. Cui, M. Q. Qi, X. Wan, J. Zhao, and Q. Cheng, "Coding metamaterials, digital metamaterials and programmable metamaterials," *Light: Sci. Appl.*, vol. 3, no. 10, p. e218, Oct. 2014.
[14] H. J. Dai, Y. J. Zhao, H. Y. Sun, J. Q. Chen, Y. Ge, and Z. Li, "An ultra-wideband linear polarization conversion metasurface," *Jpn. J. Appl. Phys.*, vol. 57, no. 9, 2018, Art. no. 090311.
[15] Y. Liu, K. Li, Y. Jia, Y. Hao, S. Gong, and Y. J. Guo, "Wideband RCS reduction of a slot array antenna using polarization conversion metasurfaces," *IEEE Trans. Antennas Propag.*, vol. 64, no. 1, pp. 326–331, Jan. 2016.
[16] J. Y. Yin, X. Wan, Q. Zhang, and T. J. Cui, "Ultra wideband polarization-selective conversions of electromagnetic waves by metasurface under large-range incident angles," *Sci. Rep.*, vol. 5, no. 1, p. 12476, Jul. 2015.
[17] H. Chen, H. Ma, S. Qu, J. Wang, Y. Li, H. Yuan, and Z. Xu, "Ultra-wideband polarization conversion metasurfaces," in *Proc. 3rd Asia–Pacific Conf. Antennas Propag.*, Jul. 2014, pp. 101–1009.